Calculations of Electron Inelastic Mean Free Paths for 31 Materials

S. Tanuma,* C. J. Powell and D. R. Penn

National Bureau of Standards, Gaithersburg, MD 20899, USA

We present new calculations of electron inelastic mean free paths (IMFPs) for 200–2000 eV electrons in 27 elements (C, Mg, Al, Si, Ti, V, Cr, Fe, Ni, Cu, Y, Zr, Nb, Mo, Ru, Rh, Pd, Ag, Hf, Ta, W, Re, Os, Ir, Pt, Au and Bi) and four compounds (LiF, SiO_2, ZnS and Al_2O_3). These calculations are based on an algorithm due to Penn which makes use of experimental optical data (to represent the dependence of the inelastic scattering probability on energy loss) and the theoretical Lindhard dielectric function (to represent the dependence of the scattering probability on momentum transfer). Our calculated IMFPs were fitted to the Bethe equation for inelastic electron scattering in matter; the two parameters in the Bethe equation were then empirically related to several material constants. The resulting general IMFP formula is believed to be useful for predicting the IMFP dependence on electron energy for a given material and the material-dependence for a given energy. The new formula also appears to be a reasonable but more approximate guide to electron attenuation lengths.

INTRODUCTION

Knowledge of the values of inelastic mean free paths (IMFPs) and attenuation lengths (ALs) for low-energy electrons in solids is important for quantitative surface analysis by AES and XPS as well as for determining the surface sensitivity of other electron-spectroscopic methods of surface characterization. Although the terms IMFP, AL and escape depth are frequently used interchangeably, each has a separate meaning.[1] The IMFP can be obtained from theory and certain types of experiments, while the AL is obtained from overlayer-film experiments and with use of a model in which the effects of elastic electron scattering are ignored. The escape depth is the product of the AL and the cosine of the angle defined by the analyzer direction and the surface normal in an AES and XPS experiment. The IMFP will be systematically larger than the AL by about 15–30%, the difference being greatest for high atomic numbers and low electron energies.[2]

One method for quantitative surface analysis by AES or XPS requires knowledge of the AL dependence on material at a given electron energy (e.g. for a 'matrix correction' of elemental sensitivity factors). Another method for quantitative analysis requires knowledge of the AL dependence on electron energy for a given material (e.g. in comparisons of peak intensities at different electron energies). Unfortunately, the AL data now available are not sufficient for many applications and, more importantly, the available data are either of uncertain or inadequate accuracy.[1] Empirical AL formulas,[3,4] which are certainly convenient and useful guides, are based on these AL data and other assumptions which limit their accuracy.[1]

We present here new calculations of IMFPs for 31 materials for electron energies between 200 and 2000

eV, part of the range of interest for many AES and XPS applications. These calculations are based on an algorithm due to Penn[5] in which experimental optical data are used to give information on the inelastic scattering probability as a function of energy loss and in which theory is used to describe the dependence of the scattering probability on momentum transfer. This hybrid approach enables us to take advantage of the available optical data (that can be checked for internal consistency by various sum rules) and avoids the necessity for making assumptions about the relative strengths of various valence-electron and core-electron excitations.[6]

The calculated IMFPs were found to be well described by the Bethe equation for inelastic electron scattering. We then found empirically that the two parameters in the Bethe equation for each material could be simply related to other material constants. These relationships have led us to a general IMFP formula which we believe will be useful for predicting IMFPs in other materials. Since AL data of the required range and accuracy are not available, the new formula is suggested as a reasonable but more approximate guide to ALs.

We describe the IMFP theory and our selection and review of the optical data which are used for the IMFP calculations. The IMFP results are presented for 27 elements and four compounds, materials for which suitable optical data were conveniently available. We describe our fits to the Bethe equation and show how we have obtained the new general formula. Our IMFP results and values from the general formula are then compared with the IMFP formula of Szajman et al.,[8] the AL formulae of Seah and Dench,[3] and the results of AL measurements. A brief account of our results has been published previously.[9]

THEORY

We describe here the Penn algorithm[5] for calculation of IMFPs which should be applicable to a wide range of

* Permanent address: Central Research Laboratories, Nippon Mining Company Ltd., 3-17-35 Niizo-Minami, Toda, Saitama 335, Japan.

materials and which, in its general form, should be useful for all electron energies. In the present work, we make use of an approximation which limits the IMFP calculation to electron energies greater than about 200 eV.

The algorithm is based on a model dielectric function for which the momentum dependence is determined by the use of the statistical approximation. The statistical approximation was first applied to IMFP calculations by Tung et al.[10] who approximated the IMFP directly whereas Penn approximated the dielectric function. The resulting model dielectric function at zero momentum transfer was equated with the measured optical dielectric function. The concept of using experimental optical data in IMFP calculations was developed by Howie and Stern, and by Powell.[6,11]

The IMFP for an electron of energy $E_k = \hbar^2 k^2/2m$ in a free-electron gas is

$$\lambda_L(k; r_s) = \left(\frac{\hbar k}{m}\right)\left(\frac{\hbar}{2|M_I(k; r_s)|}\right) \qquad (1)$$

where r_s is the average distance between valence electrons in units of the Bohr radius a_o; that is, $r_s = (\frac{3}{4}\pi n)^{1/3} a_o^{-1}$, where n is the valence electron density. The imaginary part of the electron self-energy is given by Quinn[12] as

$$M_I(k; r_s) = -\frac{e^2}{2\pi^2} \int \frac{d^3 q}{q^2} \text{Im} \frac{1}{\varepsilon_L(q, E_k - E_{k-q}; r_s)} \qquad (2)$$

$$E_k \geqslant E_{k-q} \geqslant E_F$$

where E_F is the Fermi energy and ε_L is the Lindhard dielectric function expressed as a function of momentum transfer q, energy transfer $E_k - E_{k-q}$, and r_s. This approximation neglects the vertex correction, self-consistency, exchange, and correlation, but gives reasonable values for the IMFP in free-electron-like materials.[13] A free-electron-like material is one in which the loss function $-\text{Im}[1/\varepsilon(q = 0, \omega)]$, as determined from optical or electron-energy-loss experiments, shows a dominant peak due to well-defined volume plasmons which have an energy close to the free-electron value $\hbar\omega_p = \hbar(4\pi n e^2/m)^{1/2}$. Equations (1) and (2) can be derived in a fairly simple way by calculating the scattering rate of an electron in a free-electron gas using the Born approximation.[14,15]

The dielectric function has not been calculated from first principles for non-free-electron metals such as the transition and noble metals. Consequently, (2) cannot be employed to determine the IMFP. Tung et al.[10] have used the statistical approximation developed by Lindhard and co-workers[16] to calculate the IMFP. The statistical approximation as applied to calculating the electron IMFP assumes that the inelastic scattering of an electron in a volume element $d^3 r$ of the solid can be approximated by the scattering appropriate to a free-electron gas of the electron density $n(r)$, in that volume element. Thus, the statistical approximation gives the inverse IMFP as

$$\lambda_I^{-1}(k) = \int \frac{d^3 r}{\Omega} \lambda_L^{-1}(k; r_s(r)) \qquad (3a)$$

where

$$r_s(r) = [\frac{3}{4}\pi n(r)]^{1/3} a_o^{-1} \qquad (3b)$$

and the region of integration in (3a) is a Wigner–Seitz cell of volume Ω. For simplicity, the charge distribution is assumed to be spherically symmetric and the Wigner–Seitz cell is replaced by a sphere of volume Ω.

In order to take advantage of the generally available values of $\varepsilon(\omega)$, the experimentally determined optical dielectric function, the response function $\varepsilon(q, \omega)$ of the material under consideration is approximated rather than $\lambda^{-1}(k)$. In analogy with (3a), it is assumed that

$$\text{Im} \frac{1}{\varepsilon(q, \omega)} = \int \frac{d^3 r}{\Omega} \text{Im} \frac{1}{\varepsilon_L(q, \omega; r_s^P(r))}, \qquad (4a)$$

where

$$r_s^P(r) = [\frac{3}{4}\pi n_p(r)]^{1/3} a_o^{-1} \qquad (4b)$$

Here, $n_p(r)$ is a pseudo-charge-density chosen to ensure that

$$\text{Im} \frac{1}{\varepsilon(0, \omega)} = \text{Im} \frac{1}{\varepsilon(\omega)} \qquad (5)$$

where $\varepsilon(\omega)$ is the optically measured dielectric function. In (4), a fictitious charge density $n_p(r)$ is introduced (rather than the charge density $n(r)$) in order to make use of the information contained in the experimental $\varepsilon(\omega)$. While there may be errors in the resulting functional form of $\text{Im}[1/\varepsilon(q, \omega)]$, the errors in the resulting IMFP values will be much smaller due to the later integrations over q and ω.

The integration variable in (4a) is changed from r to $\omega_p(r)$ where

$$\omega_p(r) = \left(\frac{4\pi e^2}{m} n_p(r)\right)^{1/2} \qquad (6)$$

so that (4a) becomes

$$\text{Im} \frac{1}{\varepsilon(q, \omega)} = \int_0^\infty d\omega_p\, G(\omega_p)\text{Im} \frac{1}{\varepsilon_L(q, \omega; \omega_p)} \qquad (7)$$

If q is set equal to zero and with the use of

$$\text{Im} \frac{1}{\varepsilon_L(0, \omega; \omega_p)} = -\frac{\pi}{2} \omega_p \delta(\omega - \omega_p) \qquad (8)$$

(5) yields

$$G(\omega) = -\frac{2}{\pi\omega} \text{Im} \frac{1}{\varepsilon(\omega)} \qquad (9)$$

The imaginary part of the self-energy is now obtained by replacing $\text{Im}(1/\varepsilon_L)$ in (2) by $\text{Im}(1/\varepsilon)$ in (7). The resulting equation can be written as

$$M_I(k) = -\frac{e^2}{2\pi^2} \int_0^{E_k - E_F} d(\hbar\omega) \int \frac{d^3 q}{q^2}$$

$$\times \text{Im} \frac{1}{\varepsilon(q, \omega)} \delta(\hbar\omega - E_k + E_{k-q}) \qquad (10)$$

The condition

$$\hbar\omega = E_k - E_{k-q} \qquad (11)$$

restricts the region in (ω, q) space over which the integrations in (10) take place. Equation (11) describes a collision in which an electron of energy E_k makes a transition to the state E_{k-q} and loses energy $\hbar\omega$. In this paper we assume that E_k and E_{k-q} are free-electron-like because we restrict ourselves to energies $E_k > 150$ eV.

Equation (11) then gives

$$h\omega \leq \frac{\hbar^2}{2m}(2kq - q^2) \qquad (12)$$

where k is the initial momentum of the scattered electron. Equations (7), (9) and (10) yield

$$M_1(k) = \int_0^\infty d\omega_p\, G(\omega_p)\, \frac{e^2}{2\pi^2} \int_0^{E_k - E_F} d(h\omega) \int \frac{d^3q}{q^2}$$

$$\times \mathrm{Im}\, \frac{1}{\varepsilon_L(q,\,\omega;\,\omega_p)}\, \delta(h\omega - E_k + E_{k-q}) \qquad (13)$$

The angular integrations in (13) are trivial and yield

$$M_1(k) = \int_0^\infty d\omega_p\, G(\omega_p)\left(\frac{1}{\pi a_0 k} \int_0^{E_k - E_F} d(h\omega)\right.$$

$$\left.\times \int_{q-}^{q+} \frac{dq}{q}\, \mathrm{Im}\left(\frac{1}{\varepsilon_L(q,\,\omega;\,\omega_p)}\right)\right) \qquad (14a)$$

$$q\pm = k\{1 \pm [1 - (h\omega/E_k)]^{1/2}\} \qquad (14b)$$

We find empirically that, when E_k is 200 eV or greater, the quantity $\mathrm{Im}(1/\varepsilon_L)$ in (14a) can be replaced by the single-pole approximation with a resulting loss of accuracy in the computed IMFP of less than 3%. The single-pole approximation is

$$\mathrm{Im}\, \frac{1}{\varepsilon_L(q;\,\omega;\,\omega_p)} = -\frac{\pi}{2}\, \frac{\omega_p^2}{\omega_p(q)}\, \delta(\omega - \omega_p(q)) \qquad (15a)$$

where

$$\omega_p^2(q) = \omega_p^2 + \tfrac{3}{5}[v_F(\omega_p)q]^2 + (hq^2/2m)^2 \qquad (15b)$$

and $v_F(\omega_p)$ is the Fermi velocity of a free-electron gas with plasma frequency equal to ω_p. Use of (15) in (14) yields

$$M_1(k) = \frac{1}{2\pi a_0 k} \int d(h\omega_p)\mathrm{Im}\, \frac{-1}{\varepsilon(\omega_p)}$$

$$\times \ln\left(\frac{\bar\omega_p + \bar\omega_p(q)}{\bar{q}^2} + \frac{2}{3\bar\omega_p}\right)\Bigg|_{\bar{q}_2}^{\bar{q}_1} \qquad (16)$$

where $\bar\omega_p = h\omega_p/E_F$, $\bar{q} = q/k_F$ and $\bar\omega_p^2(q) = \bar\omega_p^2 + (4/3)\bar{q}^2 + \bar{q}^4$. The quantities $\bar{q}_1$, $\bar{q}_2$ in (16) depend on $\bar\omega_p$ and are the values of $\bar{q}$ for which $\bar\omega_p(q)$ intersects the boundary of the region given by $\bar\omega < 2k\bar{q} - \bar{q}^2$ and $\bar\omega \leq \bar{k}^2 - 1$ corresponding to the limits of integration of the second and third integrals in (14a). Analytic expressions for $\bar{q}_1$ and $\bar{q}_2$ are given in Appendix A of Ref. 5. Thus, for energies E_k above 200 eV, the IMFP can be found from (16) rather than (14) and only a single integration rather than a triple integration is required.

At high incident electron energies, (16) must reduce to the Bethe[7] formula [(19) below]. In the energy range of present interest, however, there does not appear to be a simple analytic formula for $M_1(k)$.

IMFP RESULTS

We present first an analysis of the optical data on which our IMFP calculations are based. Our IMFP results are given and then analyzed in terms of the Bethe equation for inelastic electron scattering in matter. After describing important aspects of the Bethe equation, we discuss the energy dependence of our calculated IMFPs and then present a general formula for IMFPs. Finally, we compare the results of our IMFP calculations, IMFP values from the general formula, predictions of other IMFP and AL formulae, and available AL data.

Analysis of optical data

The calculation of IMFPs requires optical data over a wide photon energy range, typically 1–2000 eV, the upper limit here corresponding to the maximum electron energy for which IMFPs are to be computed. In this phase of our work, we have made IMFP calculations for materials for which the needed optical data had been tabulated over all or nearly all of the required photon energy range.[17-20]

IMFP calculations have been made for the 27 elements and four compounds listed in Table 1. For over half of these materials, there were gaps in the tabulated optical data, often in the photon energy range 40–100 eV. We have made interpolations in such cases based on

Table 1. Errors in the f-sum rule (17) and the ps-sum rule (18) for the indicated materials. Except where noted, the integrals have been evaluated for ΔE_{max} typically equal to 100 keV

Material	Error in f-sum rule (%)	Error in ps-sum rule (%)
C	15	2
Mg	13	-3
Al	12	11
Si	1	-12
Ti	-18	0
V	-20	5
Cr	-13	6
Fe	-9	9
Ni	-1	6
Cu	2	0
Y	1	4
Zr	-12	22
Nb	-14	-23
Mo	-10	-4
Ru	-13	4
Rh	-6	8
Pd	-12	-1
Ag	9	1
Hf	-4	-16
Ta	1	3
W	-1	6
Re	4	19
Os	-4	7
Ir	-5	5
Pt	0	11
Au	13	0
Bi	6	-2
LiF[a]	-26	-41
SiO$_2$[a]	-12	-21
ZnS[a]	-47	-29
Al$_2$O$_3$[a]	-13	-35

[a] ΔE_{max} in (17) is equal to 2000 eV for LiF, SiO$_2$ and ZnS and is equal to 1600 eV for Al$_2$O$_3$.
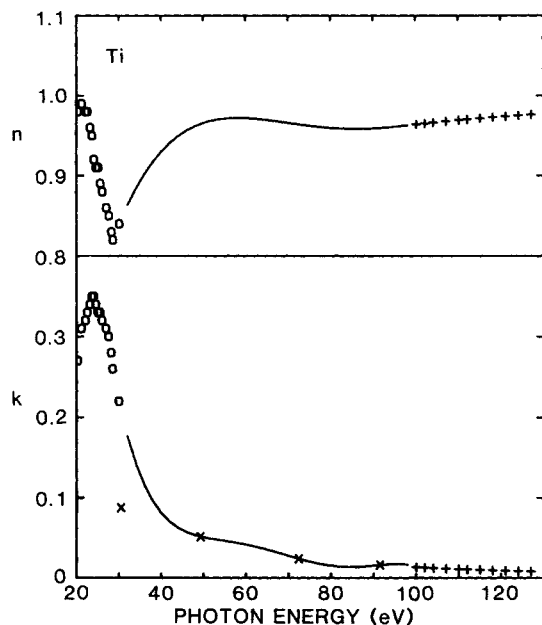
Figure 1. Example of interpolation in the optical data for titanium. The upper panel shows the refractive index n and the lower panel the extinction coefficient k as a function of photon energy: O data from Ref. 18; + data from Ref. 20; × data from Ref. 21. The solid lines are interpolations of n and k between 30 and 100 eV.

Figure 2. Plot of Z_{eff} versus ΔE_{max} from (17) for Al, Cu, Ag and Au. The horizontal arrows on the right axis show the expected values of Z_{eff} (the atomic number) when $\Delta E_{max} = \infty$.

atomic photo-absorption calculations.[21] Figure 1 shows an example of such an interpolation for titanium. The refractive index n and the extinction co-efficient $k[\varepsilon(\omega) = (n + ik)^2]$ are tabulated for photon energies between 0.1 and 30 eV in Ref. 19 and between 100 and 2000 eV in Ref. 21. The solid line in Fig. 1 shows interpolated values of n and k based on the atomic photo-absorption data for k in Ref. 21 and a calculation for n from the Kramers–Kronig dispersion relations.[22]

We have checked the internal consistency of the optical data through use of the oscillator strength (f-sum) and perfect-screening (ps-sum) sum rules.[22–24] The f-sum can be expressed as an effective number of electrons per atom or molecule Z_{eff}:

$$Z_{eff} = 2/\pi\hbar^2\Omega_p^2) \int_0^{\Delta E_{max}} \Delta E \; \mathrm{Im}[-1/\varepsilon(\Delta E)] \; d(\Delta E) \quad (17)$$
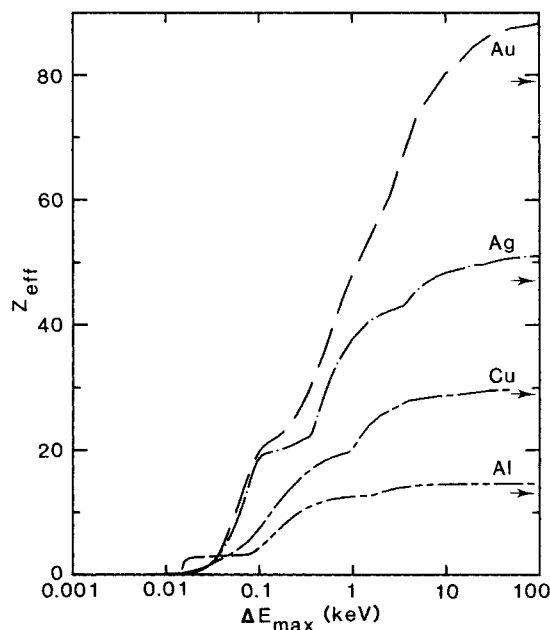
where $\Omega_p = (4\pi n_a e^2/m)^{1/2}$, $n_a = N_a\rho/A$ is the density of atoms or molecules, N_a is Avogadro's number, ρ is the bulk density, A is the atomic or molecular weight, and $\Delta E = \hbar\omega$ is the energy loss in an inelastic scattering event. When the upper limit in (17) $\Delta E_{max} = \infty$, Z_{eff} should be equal to Z, the total number of electrons per atom or molecule.

The ps-sum rule, valid only in the limit $q \to 0$, is

$$P_{eff} = (2/\pi) \int_0^{\Delta E_{max}} (1/\Delta E)\mathrm{Im}[-1/\varepsilon(\Delta E)] \; d(\Delta E) \quad (18)$$

When ΔE_{max} in (18) is equal to ∞, P_{eff} should be unity.

Figures 2 and 3 show evaluations of Z_{eff} and P_{eff} as a function of ΔE_{max} for Al, Cu, Ag and Au. The calculated values of Z_{eff} exceed the expected values (the atomic number) by 12, 2, 9 and 13 per cent, respectively. The value of P_{eff} for Al exceeds unity by 11 per cent but is close to unity for the other three metals.

Table 1 gives a listing of the errors in the f-sum and ps-sum rules, that is, the differences between the computed values of Z_{eff} and P_{eff} and those expected from (17) and (18) with $E_{max} = \infty$. While these errors are less than 10% for many materials, they can be as much as 47%. Note, however, that the generally larger errors for the four compounds in Table 1 are associated with the limited range of the available optical data and the consequently smaller value of ΔE_{max} in (17) and (18).

The errors listed in Table 1 give an indication of the likely uncertainties of the optical data. As is apparent from (17) and Fig. 2, the f-sum rule integration is influ-
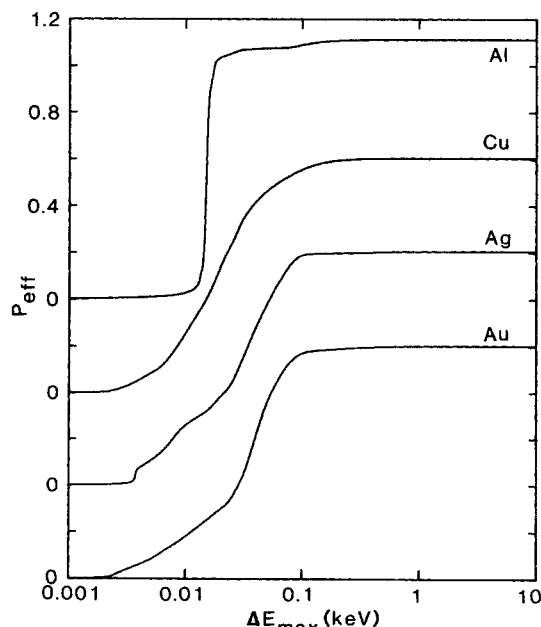
Figure 3. Plot of P_{eff} versus ΔE_{max} from (18) for Al, Cu, Ag and Au. The plots have been displaced vertically for clarity.

enced appreciably by optical data in the 50–10000 eV range; from (18) and Fig. 3, the ps-sum rule integration is influenced mainly by optical data in the 2–50 eV range. While there are a few materials in Table 1 which have small errors in both sum rules, it is not surprising that there are others that have small errors for one sum rule and large errors for the other. There are also some materials that have large errors for both sum rules. The IMFP calculation, however involves an integration of $Im[-1/\varepsilon(\omega)]$, as indicated by (16). The main contribution to this integration arises from the intermediate energies, roughly 5–100 eV. The sum rule errors in Table 1 therefore only give an approximate guide to possible errors in the resulting IMFP values; other sources of errors are discussed later.

IMFP calculations

Table 2 shows IMFP values calculated from (1) and (16) for electron energies between 200 and 2000 eV using experimental values for $Im[-1/\varepsilon(\omega)]$. We will later

compare some of these values with the results of other calculations and with AL data. The numerical values in Table 2 for Al, Cu, Ag and Au differ from those previously reported[5] because a more accurate method of numerical integration was used here.

Bethe equation for inelastic electron scattering

We introduce here the Bethe equation[7] for inelastic electron scattering since it and other related equations will be used to analyse the dependence of the calculated IMFPs on electron energy. Previous analyses[25,26] have shown that the Bethe equation provides a useful empirical description of the IMFP and AL dependences on electron energy in the range of interest for AES and XPS.

The Bethe equation for the total cross-section for inelastic scattering at an electron energy E can be written as follows:[27]

$$\sigma_{tot} = \frac{4\pi a_o^2}{(E/R)} M_{tot}^2 \ln\left(\frac{4c_{tot}E}{R}\right) \qquad (19)$$

Table 2. Calculated IMFPs (in ångströms) as a function of electron energy for 27 elements and four compounds

Electron energy (eV)	Inelastic mean free path (Å)								
	C	Mg	Al	Si	Ti	V	Cr	Fe	Ni
200	8.2	8.1	6.2	7.6	7.2	6.8	5.6	5.7	5.7
300	10.7	10.5	8.1	10.0	9.4	8.7	7.1	7.1	6.8
400	13.2	12.8	9.8	12.2	11.5	10.6	8.5	8.4	8.0
500	15.6	15.1	11.5	14.3	13.5	12.4	9.9	9.7	9.1
600	17.9	17.3	13.1	16.4	15.5	14.2	11.3	11.0	10.3
700	20.2	19.5	14.7	18.4	17.5	15.9	12.6	12.3	11.4
800	22.3	21.6	16.3	20.3	19.4	17.6	13.9	13.6	12.6
900	24.5	23.7	17.9	22.3	21.2	19.3	15.2	14.8	13.7
1000	26.6	25.7	19.4	24.2	23.1	20.9	16.5	16.1	14.8
1100	28.7	27.8	20.9	26.1	24.9	22.6	17.8	17.3	15.9
1200	30.7	29.8	22.4	27.9	26.6	24.2	19.0	18.5	16.9
1300	32.7	31.8	23.9	29.8	28.4	25.8	20.3	19.7	18.0
1400	34.7	33.7	25.4	31.6	30.1	27.3	21.5	20.8	19.1
1500	36.7	35.7	26.8	33.4	31.8	28.9	22.7	22.0	20.1
1600	38.7	37.6	28.3	35.2	33.5	30.4	23.9	23.1	21.1
1700	40.7	39.5	29.7	37.0	35.2	31.9	25.0	24.3	22.2
1800	42.6	41.4	31.1	38.8	36.8	33.4	26.2	25.4	23.2
1900	44.5	43.3	32.5	40.5	38.5	34.8	27.4	26.5	24.2
2000	46.4	45.2	33.9	42.3	40.1	36.3	28.5	27.6	25.2
	Cu	Y	Zr	Nb	Mo	Ru	Rh	Pd	Ag
200	6.4	7.4	6.5	7.5	5.5	5.1	4.9	6.2	5.3
300	7.6	9.7	8.5	9.6	7.0	6.4	6.0	7.7	6.3
400	8.9	11.8	10.4	11.6	8.4	7.7	7.3	9.3	7.5
500	10.1	13.9	12.3	13.6	9.9	9.0	8.4	10.9	8.7
600	11.3	15.9	14.0	15.5	11.3	10.3	9.6	12.4	9.8
700	12.6	17.8	15.7	17.3	12.6	11.5	10.8	13.9	10.9
800	13.8	19.7	17.4	19.1	13.9	12.7	11.9	15.3	12.1
900	15.0	21.5	19.0	20.8	15.1	13.9	13.0	16.8	13.1
1000	16.2	23.3	20.6	22.5	16.4	15.1	14.0	18.1	14.2
1100	17.4	25.1	22.2	24.2	17.6	16.2	15.1	19.5	15.2
1200	18.6	26.9	23.7	25.8	18.8	17.3	16.1	20.8	16.2
1300	19.7	28.6	25.3	27.4	20.0	18.4	17.1	22.1	17.2
1400	20.9	30.3	26.8	29.0	21.2	19.5	18.1	23.4	18.2
1500	22.0	32.0	28.3	30.6	22.3	20.5	19.1	24.6	19.1
1600	23.2	33.7	29.8	32.2	23.5	21.6	20.1	25.9	20.1
1700	24.3	35.4	31.3	33.7	24.6	22.6	21.0	27.1	21.1
1800	25.4	37.0	32.7	35.3	25.7	23.6	22.0	28.4	22.0
1900	26.5	38.7	34.2	36.8	26.8	24.6	22.9	29.6	23.0
2000	27.6	40.3	35.6	38.3	27.9	25.7	23.9	30.8	23.9

Table 2.

Electron energy (eV)	Hf	Ta	W	Re	Os	Ir	Pt	Au	Bi
				Inelastic mean free path (Å)					
200	8.0	5.4	4.9	4.2	4.9	6.4	4.9	5.0	6.9
300	10.0	6.7	6.0	5.0	5.9	7.5	5.9	5.9	8.6
400	11.9	7.9	7.2	5.9	7.0	8.8	7.0	7.0	10.3
500	13.7	9.1	8.2	6.8	8.0	10.0	8.1	8.0	12.1
600	15.5	10.3	9.3	7.6	9.0	11.2	9.1	9.0	13.7
700	17.2	11.4	10.3	8.5	10.0	12.3	10.1	10.0	15.4
800	18.8	12.6	11.3	9.3	10.9	13.4	11.1	11.0	17.0
900	20.5	13.7	12.3	10.1	11.9	14.5	12.1	11.9	18.5
1000	22.1	14.7	13.3	10.8	12.8	15.6	13.0	12.9	20.0
1100	23.7	15.8	14.2	11.6	13.7	16.7	13.9	13.8	21.5
1200	25.2	16.8	15.1	12.4	14.6	17.7	14.8	14.7	23.0
1300	26.8	17.9	16.1	13.1	15.5	18.7	15.7	15.6	24.4
1400	28.3	18.9	17.0	13.9	16.3	19.7	16.6	16.5	25.9
1500	29.8	19.9	17.9	14.6	17.2	20.7	17.5	17.3	27.3
1600	31.3	20.9	18.8	15.3	18.0	21.7	18.4	18.2	28.7
1700	32.8	21.9	19.7	16.1	18.9	22.7	19.3	19.0	30.1
1800	34.2	22.9	20.5	16.8	19.7	23.7	20.1	19.9	31.5
1900	35.7	23.8	21.4	17.5	20.6	24.7	21.0	20.7	32.8
2000	37.2	24.8	22.3	18.2	21.4	25.7	21.8	21.6	34.2

	LiF	SiO$_2$	ZnS	Al$_2$O$_3$
200	8.3	9.6	8.7	7.5
300	10.5	12.2	11.2	9.3
400	12.7	14.7	13.7	11.1
500	14.9	17.1	16.0	12.9
600	17.0	19.5	18.3	14.6
700	19.1	21.9	20.5	16.4
800	21.1	24.2	22.7	18.0
900	23.1	26.5	24.9	19.7
1000	25.1	28.7	27.0	21.3
1100	27.0	30.9	29.1	23.0
1200	29.0	33.1	31.1	24.6
1300	30.9	35.3	33.2	26.1
1400	32.8	37.4	35.2	27.7
1500	34.6	39.5	37.2	29.2
1600	36.5	41.6	39.2	30.7
1700	38.3	43.7	41.2	32.3
1800	40.1	45.7	43.1	33.8
1900	41.9	47.8	45.1	35.2
2000	43.7	49.8	47.0	36.7

where R is the Rydberg energy (13.606 eV) and M_{tot}^2 is the square of the dipole matrix element for all possible inelastic scattering processes which can be defined by

$$M_{tot}^2 = \int_0^{\Delta E_{max}} \frac{2R \, Im[-1/\varepsilon(\Delta E)] \, d(\Delta E)}{\pi \hbar^2 \Omega_p^2} \qquad (20)$$

for $\Delta E_{max} = \infty$. The term c_{tot} in (19) is a complicated function of the dependence of $Im[-1/\varepsilon(q, \omega)]$ on momentum transfer q.[27] Equation (19) is presented in its non-relativistic form, appropriate for the energy range of present interest, but can be modified to include relativistic effects if required.[27] The Bethe equation is expected to be valid for $E \gg \Delta E$; this requirement is discussed further below. Ashley[28] has shown that c_{tot} may be a function of E, but we have found no evidence for such a dependence in our analysis.

The IMFP λ_i corresponding to σ_{tot} is

$$\lambda_i = 1/n_a \sigma_{tot} \qquad (21)$$

With values for the constants inserted, (21) becomes

$$\lambda_i = \frac{AE}{28.8 \rho M_{tot}^2 \, \ln(\gamma E)} \, Å$$

$$= AE/[\alpha\rho \, \ln(\gamma E)] \, Å \qquad (22)$$

where $\gamma = 4c_{tot}/R$, energies have been expressed in eV and the density in g cm^{-3}.

Excitations of valence electrons give the major contribution to σ_{tot} in (19) and it is convenient for some applications to reformulate the Bethe equation in terms of an average excitation energy ΔE_a and a corresponding oscillator strength bN_v where N_v is the total number of valence electrons per atom or molecule and b is a parameter expected to be approximately unity.[25] In this reformulation,

$$M_{tot}^2 = RbN_v/\Delta E_a \approx RN_v/\Delta E_a \qquad (23)$$

so that (22) becomes

$$\lambda_i = \frac{2.12E}{E_p^2(b/\Delta E_a)\ln(\gamma E)} \, Å$$

$$= E/[E_p^2 \beta \, \ln(\gamma E)] \, Å \qquad (24)$$

where $E_p = 28.8(N_v\rho/A)^{1/2}$ is the free-electron plasmon energy (in eV) as indicated by (6). Equation (24) was used in our previous report.[9] Comparison of (22) and (24) yields

$$M_{tot}^2 = 28.8\beta N_v = \alpha/28.8 \qquad (25)$$

For those materials in which the dominant inelastic scattering is due to bulk-plasmon excitation (i.e. free-electron materials), $\Delta E_a = E_p = \hbar\omega_p$ and (20) can be written

$$M_{tot}^2 \approx \int_0^{\Delta E_{max}} \frac{2R\Delta E \; \mathrm{Im}[-1/\varepsilon(\Delta E)] \; d(\Delta E)}{\pi\hbar^2\Omega_p^2 E_p}$$

$$\approx RN_v/E_p \tag{26}$$

with use of (17) and where the limit ΔE_{max} has been selected to be ≈ 100 eV to emphasize the role of valence-electron excitations relevant here. Equation (26) is very similar to (23).

An important point is that the term E_p in (24) is associated with the total number of electrons (usually valence electrons but possibly including shallow core electrons in some materials) that are responsible for most of the inelastic scattering. It is possible to estimate, very approximately, the relative inelastic scattering cross-sections of valence electrons and core electrons of various binding energies.[11(b)] The core-electron cross-sections scale inversely with binding energy, as suggested by (24).[29] The term E_p thus represents the oscillator strength for those electrons that can be identified as giving the main contribution to the inelastic scattering rather than some other measure of the plasmon energy, such as the value that might be observed in an electron energy-loss experiment. The term M_{tot}^2 in (22) is similarly identified (approximately) in (23) and (26) with N_v, the total number of valence electrons responsible for the inelastic scattering. The determination of E_p or N_v should thus be based on the total number of valence electrons and of any shallow core levels with binding energies less than about 30 eV. It is the oscillator strength sum which is important in this context, not whether the material is free-electron-like or whether there is a peak identifiable as a bulk plasmon in the loss spectrum. Since there are not rigorous partial oscillator-strength sum rules for excitations associated with valence-band and core-level electrons,[22] more specific or exact guidance on the choice of N_v for particular materials cannot be given.

Dependence of IMFPs on electron energy

We have tested whether the Bethe equation (24) provides a satisfactory description of the energy dependence of the calculated IMFPs in Table 2. As before,[25,26] Fano plots were constructed by plotting values of (E/λ_i) versus ln E. If the data points lie sufficiently close to a straight line, values of the parameters β and γ in (24) can be found from a linear least-squares analysis.

For the 31 materials under consideration, linear Fano plots were found to better than 3% over the electron energy range 300–2000 eV. Over the energy range 200–2000 eV, the deviations could be up to 8%. The latter maximum deviation was considered acceptable in our search for a simple general formula that could be useful for predicting IMFPs. Examples of our Fano plots are shown in Fig. 4 for Al, Cu, Ag and Au; these plots exhibit a high degree of linearity and do not show the breaks found previously[25] (on account of the more accurate integration used in evaluating (16)).
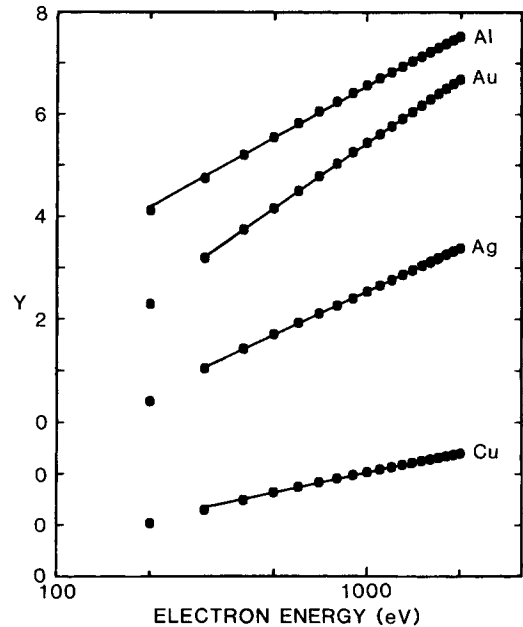
Figure 4. Fano plots for Al, Cu, Ag and Au. From (24), the function $Y = 2.12E\Delta E_a/E_p^2\lambda_i$ has been plotted *versus* electron energy on a logarithmic scale. The plots have been displaced vertically for clarity. The solid circles show values of Y based on the IMFP data in Table 2 and the solid lines show linear least-squares fits.

Table 3 lists the values of β and γ derived from our least-squares fits together with the values of N_v and E_p used in (24). We show two entries for Bi, one with $N_v = 5$ to represent the valence electrons and another with $N_v = 15$ to include also the electrons in the $O_{4,5}$ levels that have a binding energy of about 25 eV; we will comment later on the significance of these two choices.

We note here that the values of γ in Table 3 range from a low of 0.0239 for Ir to a high of 0.109 for C. It is this variation of γ that leads to different dependences of λ_i on E in the various materials.

General formula for IMFPs

Since the Bethe equation provides a satisfactory description of the dependences of the IMFP on electron energy in each of these 31 materials, we have sought simple formulae through which the parameters β and γ in (24) might be related to other material constants (such as E_p, A, ρ and N_v). We were guided in our search for a formula for β by the expectation, from (25) and (26), that β should be approximately inversely proportional to E_p. Such a relationship was found to be useful (and superior to other possible dependences that were explored) although better results were obtained with additional consideration of the bandgap energy E_g for non-conductors, as suggested by the results of Szajman *et al.*[8] Examination of the residuals also led to further improvements. Our final formulae for β and γ are

$$\beta = -2.52 \times 10^{-2} + 1.05/(E_p^2 + E_g^2)^{1/2} + 8.10$$

$$\times 10^{-4}\rho \tag{27}$$

and

$$\gamma = 0.151\rho^{-0.49} \tag{28}$$

where E_g has been expressed in eV.

Table 3. Values of β and γ found in the fits of the Bethe equation (24) or
(25) to the calculated IMFPs in Table 2; values are also given for
N_v and E_p for each material. We list values of M^2_{tot} calculated
from the optical data using (20) and from the values of β using
(25). See text for a discussion of the two entries for bismuth

Material	N_v	E_p (eV)	β (eV⁻¹ Å⁻¹)	γ (eV⁻¹)	M^2_{tot} Equation (20)	M^2_{tot} Equation (25)
C	4	20.4	0.0194	0.109	1.34	2.23
Mg	2	10.9	0.0718	0.0942	3.55	4.13
Al	3	15.8	0.0461	0.0877	3.47	3.98
Si	4	16.6	0.0332	0.0908	3.35	3.82
Ti	4	17.7	0.0304	0.0962	3.20	3.50
V	5	22.3	0.0219	0.0791	2.84	3.16
Cr	6	26.3	0.0209	0.0664	3.24	3.61
Fe	8	30.6	0.0166	0.0547	3.35	3.82
Ni	10	35.5	0.0145	0.0397	3.55	4.18
Cu	11	35.8	0.0134	0.0358	3.52	4.23
Y	3	11.2	0.0785	0.0779	6.06	6.77
Zr	4	15.4	0.0467	0.0799	4.86	5.38
Nb	5	19.6	0.0291	0.0548	3.73	4.18
Mo	6	23.0	0.0287	0.0560	4.43	4.95
Ru	8	22.6	0.0202	0.0565	4.21	4.65
Rh	9	30.0	0.0202	0.0508	4.76	5.23
Pd	10	30.6	0.0148	0.0538	3.85	4.26
Ag	11	29.8	0.0214	0.0413	5.95	6.77
Hf	4	15.7	0.0509	0.0361	4.98	5.87
Ta	5	19.5	0.0500	0.0353	6.10	7.19
W	6	22.9	0.0405	0.0348	5.96	7.00
Re	7	25.6	0.0404	0.0320	6.87	8.15
Os	8	28.1	0.0289	0.0308	5.62	6.65
Ir	9	29.7	0.0230	0.0239	5.28	5.95
Pt	10	30.2	0.0239	0.0338	5.89	6.89
Au	11	29.9	0.0248	0.0332	6.81	7.85
Bi	5	14.0	0.0648	0.0523	8.22	9.33
Bi	15	24.2	0.0216	0.0523	8.22	9.33
LiF	8	26.0	0.0133	0.0844	2.78	3.06
SiO₂	16	22.0	0.0136	0.0681	6.84	7.83
ZnS	18	25.0	0.0134	0.0819	6.14	6.95
Al₂O₃	24	27.9	0.0149	0.0570	9.05	10.3

We have compared values of β and γ calculated from
(27) and (28) for each of the 31 materials with the actual
values listed in Table 3. The resulting errors in β and γ
are plotted in Figs 5–8 against the errors in the f-sum
and ps-sum rules for each material (shown in Table 1).
These plots were made to determine whether the errors
in β and γ were associated, at least in part, with defi-
ciencies of the optical data for particular materials. No
obvious correlations were found in Figs 5–8 although,
as noted earlier, the internal-consistency checks on the
optical data given by (17) and (18) emphasize spectral
regions different from that most significant in our
IMFP calculations.

We have compared IMFP values calculated from our
general formula (24), (27) and (28) with the IMFP values
shown in Table 2 for this group of 31 materials. For any
one material, the IMFP values from the general formula
at energies between 200 and 2000 eV (100 eV intervals)
were systematically lower or higher than those listed in
Table 2. We have chosen to express the deviations
between the two sets of values for each material in
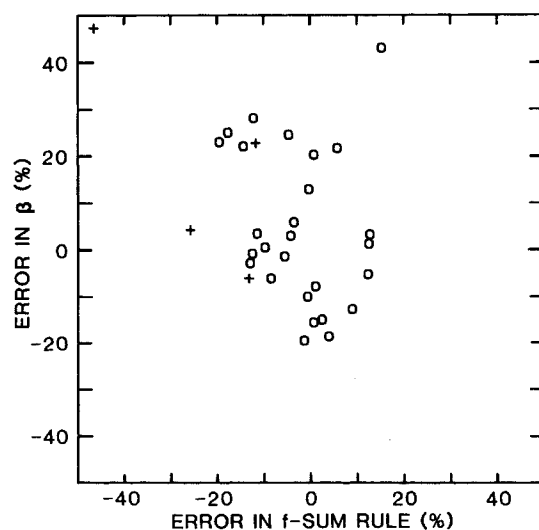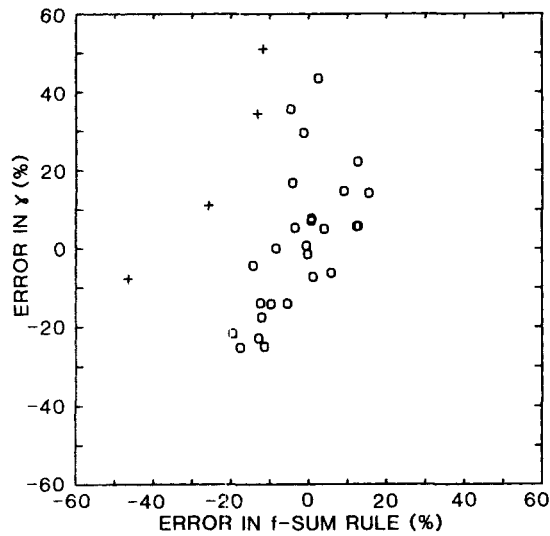terms of an RMS difference even though the differences

Figure 5. Plot of errors in β (the percentage difference between
the values calculated from (27) and the values listed in Table 3)
versus the errors in the f-sum rule (Table 1) for the 31 materials
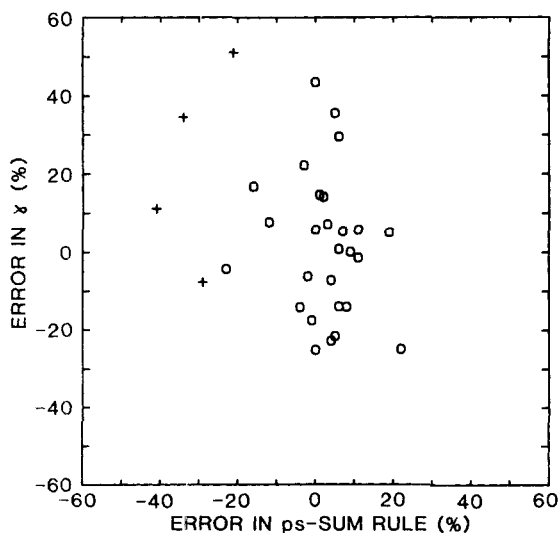(○ elements, + compounds).

Figure 6. Plot of errors in γ (the percentage difference between the values calculated from (28) and the values listed in Table 3) *versus* the errors in the f-sum rule (Table 1) for the 31 materials (○ elements, + compounds).
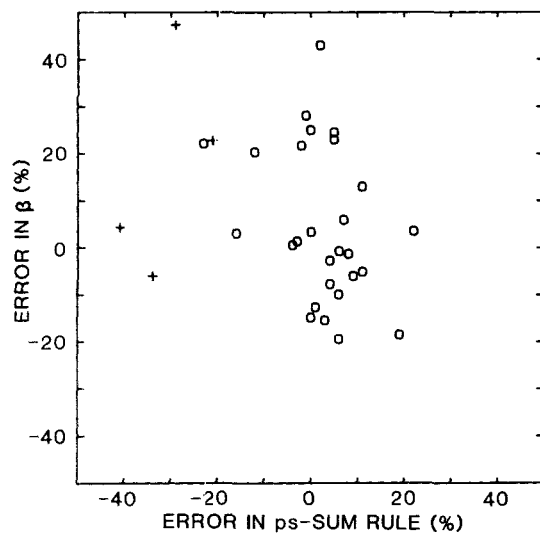
Figure 7. Plot of errors in β *versus* the errors in the ps-sum rule for the 31 materials. See caption to Fig. 4.

Figure 8. Plot of errors in γ *versus* the errors in the ps-sum rule for the 31 materials. See caption to Fig. 5.

Table 4. Root-mean-square difference between the IMFP values shown in Table 2 and the IMFP values calculated from (24), (27) and (28) and the values of E_p shown in Table 3. The sign indicates whether the IMFP values calculated with (24) are systematically lower (−) or higher (+) than the values in Table 2

Material	RMS difference (%)
C	−32
Mg	−6
Al	4
Si[a]	−19
Ti	−14
V	−14
Cr	5
Fe	6
Ni	16
Cu	6
Y	10
Zr	4
Nb	−17
Mo	4
Ru	−1
Rh	6
Pd	−18
Ag	11
Hf	−7
Ta	16
W	11
Re	21
Os	−7
Ir	−27
Pt	−11
Au	−5
Bi[b]	14
Bi[c]	−16
LiF[d]	−6
SiO$_2$[e]	−26
ZnS[f]	−31
Al$_2$O$_3$[g]	−2

[a] $E_g = 1.1$ eV
[b] $N_v = 5$
[c] $N_v = 15$
[d] $E_g = 11.8$ eV
[e] $E_g = 9.1$ eV
[f] $E_g = 3.6$ eV
[g] $E_g = 9.0$ eV

were systematic rather than random. Table 4 lists the RMS differences for our materials, the sign indicating whether the results from the general formula were higher (positive) or lower (negative) than those shown in Table 2. The maximum RMS difference in Table 4 is 32% and the average RMS difference is about 12%. These differences were not considered excessive in view of the uncertainties in the optical data (Table 1), the empirical basis for (27) and (28), and the small number of non-conductors in our data set.

Comparisons of IMFP results with other IMFP and AL data

We now present comparisons of our IMFP values, results from the general formulae (24), (27) and (28), predictions from other IMFP and AL formulae and avail-
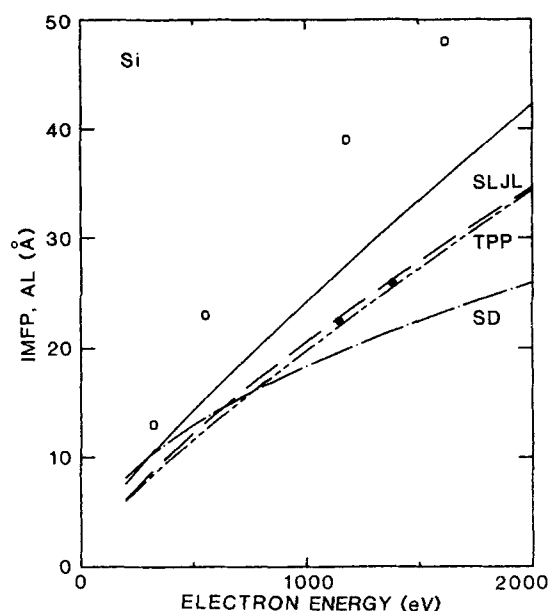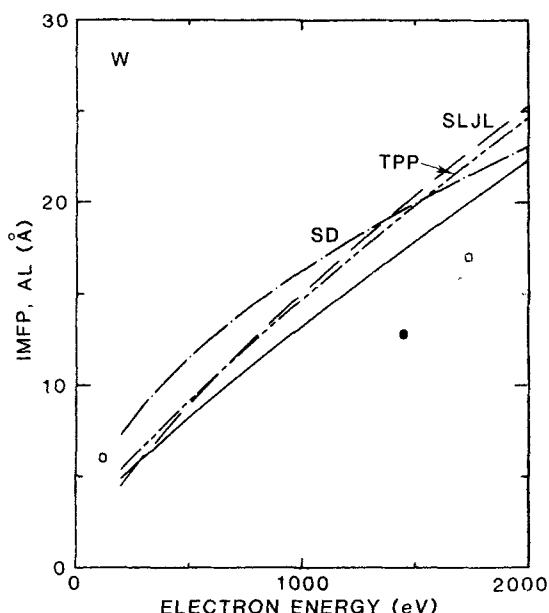
Figure 9. Comparison of IMFP and AL results for silicon. The solid line shows IMFP values calculated from (1) and (16), as listed in Table 2; the curve devoted TPP is the result of the general formula (24), (27) and (28) using parameter values for Si; the curve designated SLJL is the IMFP result of Szajman et al.,[8] (29a); and the curve denoted SD is the AL result of Seah and Dench,[3] (30). The points show experimental AL values: O, Klasson et al.;[30] ●, overlapping results of Flitsch and Raider[31] and of Ebel and Lieble.[32]

able AL measurements. Figures 9–13 show these comparisons for Si, Mo, W, SiO_2 and Al_2O_3; similar comparisons have been published previously for Al, Cu, Ag and Au.[9] The solid lines in these figures show our IMFP values (Table 2) and the curves labeled TPP indicate the results from the general formula (with parameter values appropriate for each material, as listed in Tables 3 and 4). All of the curves and most of the AL data in Figs 9–13 are for $E > 200$ eV so that the familiar minimum in λ_i is not shown.
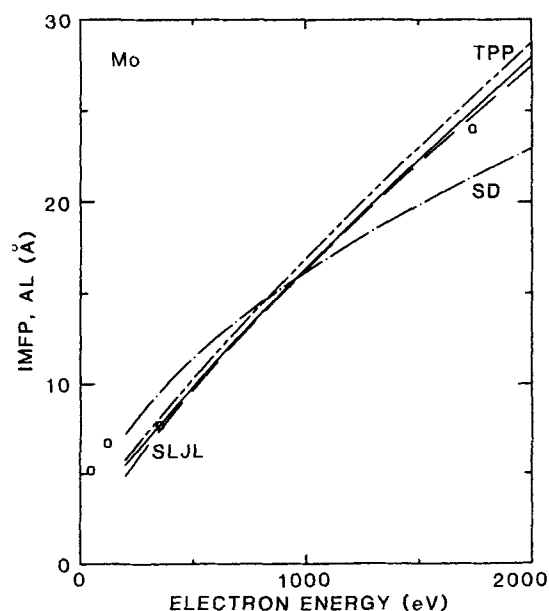
Figure 10. Comparison of IMFP and AL results for molybdenum; see caption to Fig. 9. The open circles are the AL values of Tarng and Wehner.[33]

Figure 11. Comparison of IMFP and AL results for tungsten; see caption to Fig. 9. The points show AL values: ● Carlson and McGuire;[34] O Tarng and Wehner.[33]

The curves denoted SLJL in Figs 9–13 show the simplified IMFP formula of Szajman et al.[8] for $E > 300$ eV:

$$\lambda_i \approx 1.8\bar{E}E^{3/4}/E_p{}^2 \text{ Å} \qquad (29a)$$

where $\bar{E}$ is the centroid value in the energy-loss function $Im[-1/\varepsilon(\omega)]$ in eV. For non-conductors, Szajman et al. report that $\bar{E} \approx E_p + E_g$. For free-electron-like solids, $\bar{E} \approx E_p$ and (29a) becomes

$$\lambda_i \approx 1.8E^{3/4}/E_p \text{ Å} \qquad (29b)$$

Seah and Dench[3] have analysed many AL measurements and have derived the following empirical rela-
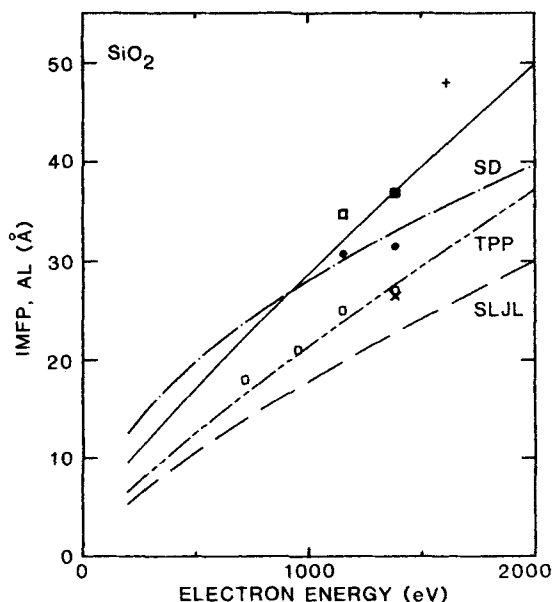
Figure 12. Comparison of IMFP and AL results for silicon dioxide; see caption to Fig. 9. The points show AL values: + Klasson et al.;[30] O Flitsch and Raider;[31] ● Ebel and Lieble;[32] ■ Hill et al.;[35] □ Ishizaka et al.;[36] and × Hattori and Nishira.[37]
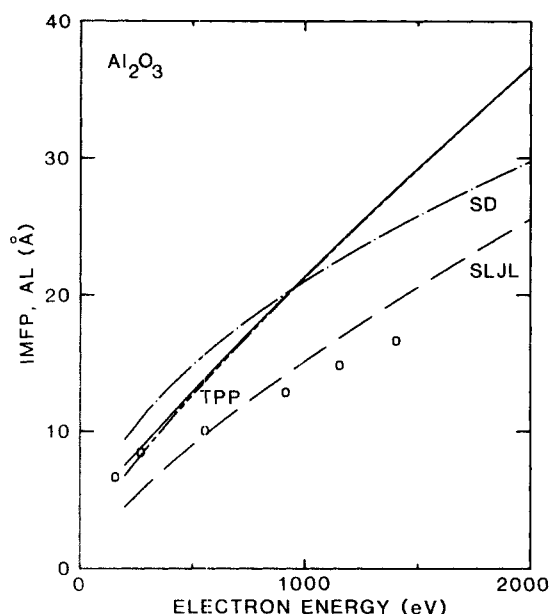
Figure 13. Comparison of IMFP and AL results for aluminium oxide; see caption to Fig. 9. The open circles are the AL values of Battye et al.[38]

tions for the AL, λ_a, for different classes of materials. They find for elements:

$$\lambda_a = 538aE^{-2} + 0.41a^{3/2}E^{1/2} \text{ nm} \qquad (30a)$$

and for inorganic compounds

$$\lambda_a = 2170aE^{-2} + 0.72a^{3/2}E^{1/2} \text{ nm} \qquad (30b)$$

where a is the average monolayer thickness (in nm) given by

$$a^3 = 10^{27}A/\rho n_A N_a \qquad (30c)$$

and n_A is the number of atoms in a molecule. The lines labeled SD in Figs 9–13 are plots of (30).

Figures 9–13 contain AL measurements for Si,[30–32] Mo,[33] W,[33,34] SiO$_2$[30–32,35–37] and Al$_2$O$_3$.[38] The newer AL measurements for Si[31,32] in Fig. 9 at 1150 and 1380 eV have been confirmed by other measurements.[36,37,39] These plots and those published earlier[9] indicate that our calculated IMFP values are comparable in magnitude to the published ALs although it is difficult to determine whether a particular result is 'correct' on account of likely systematic errors in the AL measurements or in the IMFP calculations.[1] In the relatively few cases in which replicate AL measurements have been made on the same material in different laboratories, it is not unusual to find discrepancies of up to about 100%. It is therefore hard even to confirm whether the IMFPs are systematically higher than the ALs, as expected,[2] although our plots indicate that this may be likely.

The Szajman et al.[8] formula, (29a) gives IMFP results similar in magnitude and energy dependence to our values but there are large differences in IMFP magnitudes for Cu, SiO$_2$ and Al$_2$O$_3$. A probable reason for these differences is the assumption by Szajman and Leckey[40] (whose work was the foundation for (29)) that all the valence-electron oscillator strength is associated with a single mode of energy loss. In reality, there is oscillator strength distributed over other energy-loss

modes that reduces the single-mode loss intensity and which has the net effect of reducing the total inelastic scattering cross-section or increasing the IMFP. Our use of the energy-loss function allows us to include all energy-loss modes, properly weighted, for both valence and core electrons. Our IMFP values for Cu, SiO$_2$ and Al$_2$O$_3$ (and also for Al, Ni, Ag and Au) agree well with those published by Ashley et al.[10,41]

Our IMFP values are similar to the AL results from the Seah and Dench formula (30) for most materials. The energy dependence of (30), however, is rather different than we find for most of our IMFP results.

Figures 9–13 also show graphically the degree of correspondence between our IMFP values and the results given by (24), (27) and (28). Even for a material such as SiO$_2$ which has a 26% difference between results from our calculations and our general formula, Fig. 12 indicates that this difference is, unfortunately, not significantly worse than the variability in AL results.

DISCUSSION

Our IMFP calculations are based on the assumption that the Born approximation is valid and on the neglect of vertex corrections, self-consistency, exchange and correlation.[5] For $E > 200$ eV, these assumptions are estimated to introduce errors of the order of 10% for free-electron-like materials; for other materials, the errors could be larger. Another source of uncertainty arises from approximations leading to (7). We do in fact obtain quantitatively reasonable IMFP values since inelastic electron scattering occurs predominantly in the forward direction, with small momentum transfer, so that the dependence of the inelastic scattering probability on energy loss is closely related to $\text{Im}[-1/\varepsilon(0, \omega)]$. The q-dependence of $\text{Im}[-1/\varepsilon(q, \omega)]$ is not well known for non-free-electron-like materials, however, and it is difficult to estimate the errors associated with our use of the single-pole approximation in (15). The latter approximation limits our present IMFP calculation to electron energies above 200 eV but we are planning in the future to compute IMFPs with (14) which should yield valid results for energies above about 50 eV.

The calculated IMFP values are expected to have errors due to uncertainties in the experimental optical data. As discussed earlier, errors in the sum rules for the dielectric function (such as those presented in Table 1) give an indication of the overall quality of the optical data. The sum rule errors should not, however, be considered necessarily as IMFP errors since the IMFP calculation using (16) emphasizes optical data in the vicinity of 5–100 eV. Large errors in the sum rules do not directly lead to large IMFP errors nor do small sum rule errors necessarily suggest small IMFP errors. Figures 5–8 do not show any correlation between sum rule errors and errors in β and γ (the differences between values calculated from (27) and (28) and those listed in Table 3). The RMS sum rule errors are comparable to the RMS value of the errors listed in Table 4 between the IMFP values calculated here and those obtained from the general formula and, given the empirical nature of (27) and (28) and the uncertainties of the model, it was not judged useful to seek higher accuracy.
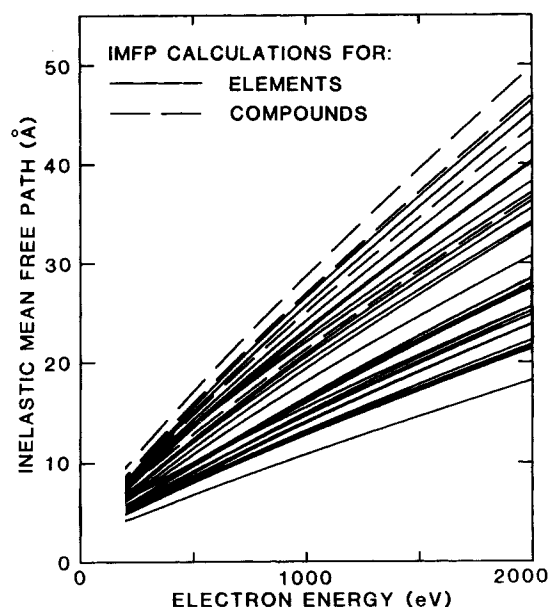
Figure 14. Plots of IMFPs *versus* electron energy for the 27 elements (solid lines) and four compounds (dashed lines).

The total uncertainties arising from the approximations in our IMFP algorithm are likely to be systematic; the IMFP results in Table 2 may thus be systematically high or low compared to the true values. Nevertheless, we believe that we can determine with reasonable accuracy both the IMFP material dependence at particular electron energies and the IMFP energy dependence for particular materials.

Figure 14 shows a summary plot of our calculated IMFPs for the 27 elements and four compounds as a function of electron energy. At any energy, the ratio of the largest IMFP to the smallest IMFP is about 2.5. We expect that a larger range of IMFPs would be found if materials of lower density (e.g. polymers and alkali metals) had been included. While we have been able here to calculate IMFPs for about a third of the solid elements, we have so far computed IMFPs for only four compounds. We hope to remedy this deficiency shortly but, in the meantime, Fig. 14 should not be used to indicate a typical IMFP range for compounds.

Our general IMFP formula, (24), (27) and (28), summarizes in compact form the IMFP dependences on material and electron energy. The material dependence in this formula occurs principally through the parameter β and to a lesser extent through the parameter γ. Our strategy in developing this formula was to use as much physical information available as possible. The Bethe equation for inelastic electron scattering is expected to be valid at 'sufficiently high' electron energies; the parameter β is then simply related to dielectric data, as indicated by (20) and (25), and the parameter γ is, in principle, calculable from theory.[27,28] Previous analyses[25,26] have shown that the Bethe equation is empirically valid for both IMFP and the AL data over an energy range of typically 100-2000 eV but that the values of β in the AL analysis are higher and those of γ lower than expected. While AL and IMFP values for a given material may be of comparable value, there could be differences in the values of β and γ for each set of data in the energy range of interest for AES and XPS.

That is, for $E < 2000$ eV, the energies are not high enough for β and γ to have attained their asymptotic values.

Detailed examination of the Fano plots (such as in Fig. 4) shows small changes of slope as a function of electron energy. The average slopes over the 200-2000 eV energy range yield values of M_{tot}^2 from (25) that for most of the materials exceed the M_{tot}^2 values expected from the optical data via (20), by about 10-20%, as indicated in Table 3. The only exception is for carbon; here, the value of M_{tot}^2 from (20) has been calculated with a density of 1.5 g cm^{-3}, as reported with the optical data,[17] although the actual density might be higher (e.g. 1.8-2.1 g cm^{-3}) and the apparent discrepancy in Table 3 would then be less. The Fano plots do not reach their asymptotic slopes until $E \gtrsim 5$ keV. The general formula, (24), (27) and (28), should therefore not be used for electron energies outside the range 200-2000 eV.

Both (27) and (28) are empirical in that they result from least-squares fits of the values of β and γ for our 31 materials (Table 3) to selected material parameters and to various combinations of these parameters. We expected (from (25) and (26)) that β should be approximately inversely proportional to E_p; the additional terms in (27) led to better least-squares fits. Since only five non-conductors are included in this analysis, it is possible that IMFP calculations for additional non-conductors may lead to modifications to (27).

For free-electron-like materials, it would be expected that γ should be inversely proportional to E_p. Indeed, (28) shows an inverse dependence close to the square root of the density, but we were not able to find a better dependence involving (A/N_v) although many of our materials are non-free-electron-like.

The material-dependence of γ (Table 3 and (28)) leads to an IMFP energy dependence that is material-dependent. The range of γ values in Table 3 (0.0239 to 0.109) is qualitatively similar to the range found in an analysis of AL data[26] for nine materials (0.005 to 0.067) and to the range found from an analysis of IMFP data[25] for Al, Cu, Ag and Au (0.024 to 0.13). The quantitative difference in γ-values for IMFP and AL data is due to the fact that the electron energies are not high enough to be in the asymptotic regime in the AL measurements. The material-dependence of γ originates from differing spectral distributions of the energy-loss functions, $\text{Im}[-1/\varepsilon(\omega)]$, for different materials and overcomes a deficiency of the Szajman *et al.*[8] and Seah and Dench[3] formulae (29) and (30).

We now comment further on the choice of N_v in the calculation of E_p for (24). Table 3 contains two extreme choices of N_v for Bi. If N_v is chosen to be 5, the number of valence electrons, $E_p = 14.0$ eV, and the value of β calculated from (27) is 0.0577, a value 11% lower than that found from the fit to the calculated IMFPs for Bi. If, however, N_v is chosen to be 15 (including the 10 5d electrons), $E_p = 24.2$ eV, and the value of β from (27) is found to be 0.0261, a value 21% higher than that found in the fit to the Bi IMFPs. Despite the large range in the choice of N_v (which corresponds to the limits in the likely oscillator strength contributing to the inelastic scattering), the resulting values of β do not differ greatly. The IMFP values calculated using (24) correspondingly do not differ substantially from the IMFP

values for Bi listed in Table 2, as shown in Table 4.

While our general IMFP formula is empirical, as described above, it is based on the well-established Bethe equation. Since this equation has a sound physical basis, we believe the general formula could be successfully utilized with other materials. No substantial difference, like that between (30a) and (30b) for elements and inorganic compounds, is to be expected. Modifications may, however, be made to our formula as we perform IMFP calculations for additional materials, particularly compounds, and extend the calculations to lower electron energies through use of (14).

The difference between IMFP and AL values for a given material may only be about 15–30%.[2] Differences of this magnitude are less than the errors likely in many AL measurements. While the absolute error in our IMFP calculations is not well known, we believe our general IMFP formula should be a useful guide to AL values required in quantitative analysis by AES or XPS.

Specifically, our formula gives information on the material-dependence and energy-dependence of the IMFP that we consider more reliable than that given by the IMFP formula of Szajman et al.[8] or the AL formula of Seah and Dench.[3] It would clearly be very useful to have an algorithm through which IMFPs from our general formula could be converted to ALs.

SUMMARY

We have presented new IMFP values for 200–2000 eV electrons in 27 elements and four compounds that have been calculated using an algorithm due to Penn.[5] Our IMFP results for each material were satisfactorily fitted to the Bethe equation for inelastic electron scattering in matter and the two Bethe parameters were empirically related to several material constants (number of valence electrons, bulk density, atomic or molecular weight and band-gap energy for non-conductors). We have thus obtained a general IMFP formula which is reliable, in comparisons to our IMFP values, to an average uncertainty of 12%. We believe this general IMFP formula is a useful guide for predicting the IMFP dependence on electron energy for a given material and the material-dependence for a given energy.

IMFP values are expected to exceed electron attenuation lengths for a given material by up to about 15–30%,[2] the difference being greatest for high atomic numbers and low electron energies. We therefore suggest that our general IMFP formula should be a useful but less accurate guide to ALs, particularly for giving information on the AL dependences on material and energy needed for quantitative surface analysis by AES and XPS. Further work is required to extend our formula to electron energies below 200 eV and above 2000 eV. IMFP calculations are also needed for additional compounds to ensure that the IMFP formula is reliable for a wide range of materials.

REFERENCES

1. C. J. Powell, J. Electron Spectrosc. (in press).
2. S. Tougaard (personal communication); A. Jablonski, Surf. Science 188, 164 (1987).
3. M. P. Seah and W. A. Dench, Surf. Interface Anal. 1, 2 (1979).
4. C. D. Wagner, L. E. Davis and W. M. Riggs, Surf. Interface Anal. 2, 53 (1980).
5. D. R. Penn, Phys. Rev. B35, 482 (1987).
6. C. J. Powell, Surf. Interface Anal. 7, 263 (1985).
7. H. Bethe, Ann. der Physik 5, 325 (1930).
8. J. Szajman, J. Liesegang, J. G. Jenkin and R. C. G. Leckey, J. Electron Spectrosc. 23, 97 (1981).
9. S. Tanuma, C. J. Powell and D. R. Penn, Surf. Science 192, L849 (1987).
10. C. J. Tung, J. C. Ashley and R. H. Ritchie, Surf. Science 81, 427 (1979).
11. (a) A. Howie and R. M. Stern, Z. Naturforsch 27a, 382 (1972); (b) C. J. Powell, Surf. Science 44, 29 (1974).
12. J. J. Quinn, Phys. Rev. 126, 1453 (1962).
13. D. R. Penn, Phys. Rev. B13, 5248 (1976).
14. R. H. Ritchie, Phys. Rev. 114, 644 (1959).
15. D. Pines and P. Nozieres, Quantum Liquids, Vol. 1, p. 308, W. A. Benjamin, New York (1966).
16. J. Lindhard and M. Scharff, Kong. Danste Vidensk. Selsk. Mat.-Fys. Medd. 27, No. 15 (1953); J. Lindhard, M. Scharff and H. E. Schiott, ibid. 33, No. 14 (1963).
17. H.-J. Hagemann, W. Gudat and C. Kunz, Deutsches Elektronen-Synchrotron Report SR-74/7, Hamburg (1974), unpublished; H.-J. Hagemann, W. Gudat and C. Kunz, J. Opt. Soc. Am. 65, 742 (1975).
18. J. H. Weaver, C. Krafka, D. W. Lynch and E. E. Koch, Optical Properties of Metals, Physik Daten, Physics Data, Nos. 18–1 and 18–2, Fachinformationszentrum, Karlsruhe (1981).
19. Handbook of Optical Constants of Solids, ed. E. D. Palik, Academic Press, New York (1985).
20. B. L. Henke, P. Lee, T. J. Tanaka, R. L. Shimabukuro and B. K. Fujikawa, in Low Energy X-ray Diagnostics, eds. D. T. Attwood and B. L. Henke, p. 340, Amer. Inst. Phys. Conf.

Proc. No. 75, American Institute of Physics, New York (1981).
21. B. L. Henke, P. Lee, T. J. Tanaka, R. L. Shimabukuro and B. K. Fujikawa, Atomic Data 27, 1 (1982).
22. D. Y. Smith, in Ref. 19, p. 35.
23. Ref. 15, p. 210.
24. G. D. Mahan, Many-Particle Physics, p. 460, Plenum, New York, 1981.
25. C. J. Powell, Surf. Interface Anal. 10, 349 (1987).
26. C. J. Powell, Surf. Interface Anal. 7, 256 (1985).
27. M. Inokuti, Rev. Mod. Phys. 43, 297 (1971).
28. J. C. Ashley, J. Electron Spectrosc. 28, 117 (1982).
29. C. J. Powell, in Electron Impact Ionization, eds. T. D. Märk and G. H. Dunn, pp. 198–231, Springer-Verlag, New York (1985).
30. M. Klasson, A. Berndtsson, J. Hedman, R. Nilsson, R. Nyholm and C. Nordling, J. Electron Spectrosc. 3, 427 (1974).
31. R. Flitsch and S. I. Raider, J. Vac. Sci. Tech. 12, 305 (1975).
32. M. F. Ebel and W. Lieble, J. Electron Spectrosc. 16, 463 (1979).
33. M. L. Tarng and G. K. Wehner, J. Appl. Phys. 44, 1534 (1973).
34. T. A. Carlson and G. E. McGuire, J. Electron Spectrosc. 1, 161 (1972).
35. J. M. Hill, D. G. Royce, C. S. Fadley, L. F. Wagner and F. J. Grunthaner, Chem. Phys. Letters 44, 225 (1976).
36. A. Ishizaka, S. Iwata and Y. Kamigaki, Surf. Science 84, 355 (1979).
37. T. Hattori and T. Nishira, Surf. Science 86, 555 (1979).
38. F. L. Battye, J. G. Jenkin, J. Liesegang and R. C. G. Leckey, Phys. Rev. B9, 2887 (1974).
39. T. Hattori and T. Suzuki, Appl. Phys. Letters 43, 470 (1983).
40. J. Szajman and R. C. G. Leckey, J. Electron Spectrosc. 23, 83 (1981).
41. J. C. Ashley, C. J. Tung and R. H. Ritchie, IEEE Trans. on Nucl. Science NS-22, 2533 (1975); J. C. Ashley and V. E. Anderson, J. Electron Spectrosc. 24, 127 (1981).